Journal of Computational Physics **160,** 283–297 (2000)
doi:10.1006/jcph.2000.6462, available online at http://www.idealibrary.com on IDEAL®

Expansion Functions for Two-Dimensional Incompressible Fluid Flow in Arbitrary Domains

J. P. Goedbloed

FOM-Institute for Plasma Physics 'Rijnhuizen,' Association Euratom-FOM, 3439MN Nieuwegein, The Netherlands
E-mail: goedbloed@rijnh.nl

Received August 10, 1999; revised January 27, 2000

Expansion functions are presented for two-dimensional incompressible fluid flow in arbitrary domains that optimally conserve the 2D structure of vortex dynamics. This is obtained by conformal mapping of the domain onto a circle and by constructing orthogonal radial polynomials and angular harmonics on the new domain such that the kinetic energy is diagonal and the separate components satisfy all of the required physical boundary conditions.

Key Words: orthogonal polynomials; conformal mapping; incompressible flow; vortex dynamics.

1. INTRODUCTION

The immediate reason for this paper is two fairly recent publications on spectral calculations of vortex dynamics of two-dimensional incompressible flow in circular domains [1]. The spectral representations exploited in those papers consist of products of orthogonal polynomials for the radial direction and harmonic functions for the angular direction. The polynomials are constructed on the basis of an inner product that is called "natural" and that leads to a special class of Jacobi polynomials which is described in detail. Apparently, Verkley is not aware of similar sets of expansion functions that were derived by the present author in 1974 for the purpose of high-beta stability calculations and extensively used since then for stability problems of a variety of configurations [2–7], including that of the joint European torus [8]. The reason may be that the stress in the mentioned publications was on results rather than methods. In particular, the expansion functions developed were only mentioned in passing, although somewhat more extensively in Ref. [7], but never discussed in detail. More important for the present purpose is that the functions turned out to be quite effective for the tokamak stability calculations since they were constructed on the basis of

0021-9991/00 $35.00

completely different choices for the inner product and the boundary conditions than those made in Ref. [1]. Also, they allowed for straightforward generalisation to arbitrary domains. Because of the present interest in vortex dynamics in two dimensions, it appears appropriate to make these methods available for wider applications than tokamak stability theory alone.

2. INCOMPRESSIBLE TWO-DIMENSIONAL FLOW

2.1. *Basics*

Exploiting cylindrical coordinates (r, θ, z), incompressible fluid flow in two dimensions $(\partial/\partial z = 0)$ is represented by

$$\nabla \cdot \mathbf{v} = \frac{\partial v_r}{\partial r} + \frac{1}{r}\frac{\partial v_\theta}{\partial \theta} = 0, \quad v_z = 0, \tag{1}$$

so that the two velocity components in the transverse plane may be derived from a single stream function $S = S(r, \theta, t)$:

$$\mathbf{v} = \mathbf{e_z} \times \nabla S, \quad \text{i.e., } v_r = -\frac{1}{r}\frac{\partial S}{\partial \theta}, \quad v_\theta = \frac{\partial S}{\partial r}. \tag{2}$$

The most important dynamical variable is the vorticity, which turns out to be the Laplacian of the stream function:

$$\omega \equiv \mathbf{e_z} \cdot \nabla \times \mathbf{v} = \nabla^2 S = \frac{1}{r}\frac{\partial}{\partial r} r \frac{\partial S}{\partial r} + \frac{1}{r^2}\frac{\partial^2 S}{\partial \theta^2}. \tag{3}$$

Its advection is given by

$$\frac{\mathrm{D}\omega}{\mathrm{D}t} \equiv \frac{\partial \omega}{\partial t} + \mathbf{v} \cdot \nabla \omega = \frac{\partial \omega}{\partial t} + \mathbf{e_z} \cdot \nabla S \times \nabla \omega \equiv \frac{\partial \omega}{\partial t} + \{S, \omega\}, \tag{4}$$

where another quantity of interest appears, viz. the Poisson bracket for arbitrary functions $F(r, \theta)$ and $G(r, \theta)$:

$$\{F, G\} \equiv \mathbf{e_z} \cdot (\nabla F \times \nabla G) = \frac{1}{r}\left(\frac{\partial F}{\partial r}\frac{\partial G}{\partial \theta} - \frac{\partial F}{\partial \theta}\frac{\partial G}{\partial r} \right). \tag{5}$$

Clearly, numerical calculation of incompressible two-dimensional flow should pay particular attention to an accurate representation of the stream function and its derivatives as appearing in the Laplacian and the Poisson brackets. Moreover, even though the problem has been reduced to a single scalar unknown S, it is important to recall that the actual physics involves the velocity vector $\mathbf{v}$. We will see that this more or less determines how the representation of the stream function in expansion functions should be chosen. Since we are not concerned with the actual calculation of the dynamics in this paper, from now on we will suppress the dependence on time in $S = S(r, \theta, t)$.

Potential, i.e., incompressible and irrotational flow on an arbitrary domain in two dimensions, is basically solved by finding the conformal mapping to the unit disk. Obviously, vortical flow in an arbitrary domain is not solved that easily, but conformal mapping of the boundary to a circle greatly facilitates the solution by means of the fast Fourier transform (FFT). We relegate the discussion on how such a mapping is obtained to Section 2.2 and

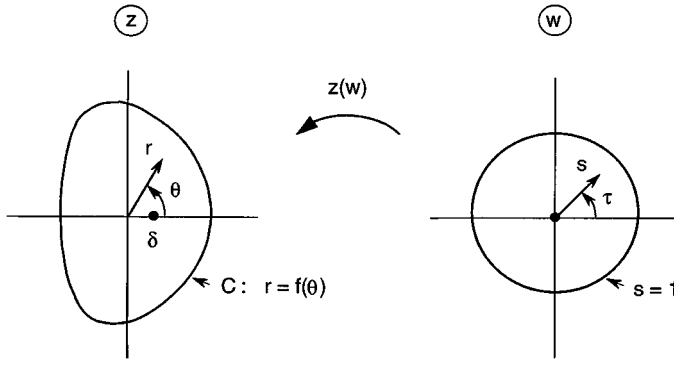

FIG. 1. Conformal mapping of an arbitrary domain bounded by the curve C in the physical z-plane to the unit disk in the computational w-plane where $w = 0$ is the image of an arbitrary interior point $z = \delta$. This mapping is produced by an explicit Moebius transformation followed or preceded by a numerical Henrici transformation.

assume that $z = z(w)$ is known. Here, z represents the physical plane where the flow is supposed to be bounded by an arbitrary curve C enclosing the origin and w represents the mapped plane where the image of the fluid domain is the unit disk $|w| \le 1$ (see Fig. 1). We introduce polar coordinates s, τ in the w-plane, i.e., $w = se^{i\tau}$, and choose the computational grid $\{w_{ij}\}$ to be, e.g., equidistant in s and τ:

$$w_{ij} = s_i e^{i\tau_j}, \begin{cases} s_i = i/I, & i = 0, 1, \dots I, \\ \tau_j = (j/J)2\pi, & j = 0, 1, \dots J-1. \end{cases} \tag{6}$$

Of course, the procedure is limited to reasonable boundary curves C so that an acceptable spacing of the grid $z(w_{ij})$ in the physical plane is obtained.

Once the conformal mapping $z = z(w)$ is known, virtually all that is needed is the scale factor h appearing in derivatives:

$$h = h(s, \tau) = \left| \frac{dz}{dw} \right|. \tag{7}$$

E.g., the velocity components corresponding to Eq. (2) become

$$v_s = -\frac{1}{hs}\frac{\partial S}{\partial \tau}, \quad v_\tau = \frac{1}{h}\frac{\partial S}{\partial s}, \tag{8}$$

and the vorticity becomes

$$\omega = \nabla^2 S = \frac{1}{h^2}\left(\frac{1}{s}\frac{\partial}{\partial s}s\frac{\partial S}{\partial s} + \frac{1}{s^2}\frac{\partial^2 S}{\partial \tau^2}\right), \tag{9}$$

whereas the Poisson bracket transforms to

$$\{F, G\} = \frac{1}{h^2 s}\left(\frac{\partial F}{\partial s}\frac{\partial G}{\partial \tau} - \frac{\partial F}{\partial \tau}\frac{\partial G}{\partial s}\right). \tag{10}$$

Clearly, the conformal mapping conserves all the basic structures needed in vorticity dynamical calculations.

Since the computational domain is now circular, the stream function may be represented as a series of products of one-dimensional radial expansion functions $R_{mn}(s)$ and angular harmonics $e^{im\tau}$,

$$S = S(s,\tau) = \sum_{m=-\infty}^{\infty} \sum_{n=0}^{\infty} \sigma_{mn} R_{mn}(s) e^{im\tau}, \tag{11}$$

where simple boundary conditions will be imposed on $R_{mn}(s)$ at $s = 0$ and $s = 1$. Consequently, all information on the stream function is now contained in the set of expansion coefficients $\{\sigma_{mn}\}$. Here, and in the following, we write infinite sums leaving it understood that they are of course truncated in the numerics to some manageable size. Before we discuss the choice of the set of appropriate functions $R_{mn}(s)$, we will first summarize the main steps in the numerical construction of the conformal mapping.

2.2. *Construction of the Conformal Mapping*

Conformal mapping of circular and elongated domains were extensively exploited in studies of high-beta tokamak equilibrium and stability [2–8]. In particular, in Ref. [4], the numerical methods involved were described in detail. Hence, we here just summarize the main ideas needed for the present purpose.

When the boundary curve C is already a circle and we just wish to map the interior onto itself but move an arbitrary point $z = \delta$ onto the origin $w = 0$, a Moebius transformation is all that is required:

$$z_1(w) = \frac{\delta + w}{1 + \delta w}. \tag{12}$$

The scale factor for this mapping is given by

$$h(s,\tau) = \frac{1 - \delta^2}{1 + \delta^2 s^2 + 2\delta s \cos\tau}. \tag{13}$$

This simple transformation was used in the mentioned studies of tokamaks with a circular cross section to move the image of the magnetic axis onto the origin. Such a simple, but crucial, device could also be of interest for studies of vorticity dynamics, e.g., in the presence of eccentric forcing. When the boundary curve C is not a circle, conformal mapping of the enclosed domain in the z-plane onto a circle in the w-plane leaving the origin invariant is effected by a transformation that may be represented as an infinite series:

$$z_2(w) = \sum_{m=1}^{\infty} \varphi_m w^m. \tag{14}$$

For simplicity, we here restrict the discussion to up–down symmetric boundary curves so that the coefficients φ_m are real. A numerical approximation of this mapping for starlike domains (radial lines emanating from the origin intersect the boundary only once) is obtained by means of an extremely elegant and effective method that has grown over many years from contributions of Theodorsen [9], Gutknecht [10], and Henrici [11, 12]. More advanced algorithms, not requiring the domain to be starlike, are discussed as well in Ref. [11]. To map an arbitrary boundary curve while also shifting the origin, the two mappings $z_1(w)$ and

$z_2(w)$ may be applied in succession, either as $z_2(z_1(w))$, involving an intermediate boundary curve C', or as $z_1(z_2(w))$, involving an intermediate shift δ'. Except for numerical accuracy, these two mappings should produce identical results.

We will now discuss how the numerical approximation of the coefficients $\{\varphi_m\}$ of the conformal mapping $z_2(w)$ is obtained, where we will drop the subscript 2. Consider an analytic function $F = F(w) = \Phi(s, \tau) + i\Psi(s, \tau)$, so that Φ and Ψ are conjugate harmonic functions. On the unit circle,

$$F(e^{i\tau}) = \phi(\tau) + i\psi(\tau), \tag{15}$$

so that the boundary functions $\phi(\tau) \equiv \Phi(1, \tau)$ and $\psi(\tau) \equiv \Psi(1, \tau)$ satisfy the Hilbert transform

$$\psi(\tau) = C_0 + \frac{1}{\pi}\mathcal{P}\oint K(\tau - \tau')\phi(\tau')\,d\tau', \quad K \equiv \frac{1}{2}\cot\frac{1}{2}(\tau - \tau'), \tag{16}$$

where C_0 is a constant. Now choosing $F(w) \equiv \ln[z(w)/w]$, these two functions become

$$\phi(\tau) \equiv \ln f(\theta(\tau)), \quad \psi(\tau) \equiv \theta(\tau) - \tau, \tag{17}$$

where $r = f(\theta)$ is the boundary curve C indicated in Fig. 1. Hence, the Hilbert transform (16) yields Theodorsen's nonlinear integral equation [9]:

$$\theta(\tau) = \tau + \frac{1}{\pi}\mathcal{P}\oint K(\tau - \tau')\ln f(\theta(\tau'))\,d\tau'. \tag{18}$$

This equation was exploited in early studies of wing design. Its (iterative) solution converges to the required boundary correspondence function $\theta = \theta(\tau)$, which is all that is needed to fix the conformal mapping $z(w)$.

Henrici showed that the iterative solution of Theodorsen's integral equation really becomes a trifle by the exploitation of FFTs. This results from the identity character of the Fourier expansion of the kernel K:

$$K(\tau - \tau') = \sum_{m=1}^{\infty} \sin m(\tau - \tau'). \tag{19}$$

This implies that the Fourier coefficients $\{a_m^{(n)}\}$ appearing in the (n)th step of the solution of the boundary function,

$$\ln f\left(\theta^{(n)}(\tau)\right) = \frac{1}{2}a_0^{(n)} + \sum_{m=1}^{\infty} a_m^{(n)} \sin m\tau, \tag{20}$$

and the Fourier coefficients $\{b_m^{(n+1)}\}$ appearing in the $(n+1)$th step,

$$\theta^{(n+1)}(\tau) - \tau = \sum_{m=1}^{\infty} b_m^{(n+1)} \sin m\tau, \tag{21}$$

are connected through the identity transformation:

$$b_m^{(n+1)} = a_m^{(n)} \quad (m \neq 0). \tag{22}$$

Hence, the iterative solution of Theodorsen's equation is obtained by means of what could be called a fast Hilbert transform, i.e., two fast Fourier transforms in succession:

$$\rightarrow \left\{ \ln f\left(\theta^{(n)}(\tau_i)\right)\right\} \xrightarrow{\text{FFT}^-} \left\{a_m^{(n)}\right\} \xrightarrow{\text{I}} \left\{b_m^{(n+1)}\right\} \xrightarrow{\text{FFT}^+} \left\{\theta^{(n+1)}(\tau_i) - \tau_i\right\} \rightarrow \tag{23}$$

Once $\theta(\tau)$ is known, i.e., the mapping is known on the boundary, the coefficients $\{\varphi_m\}$ may be obtained again by fast Fourier transformation,

$$z(e^{i\tau}) = f(\theta(\tau))e^{i\theta(\tau)} \xrightarrow{\text{FFT}^-} \{\varphi_m\}, \tag{24}$$

so that the conformal mapping $z(w)$ is known everywhere.

In the tokamak stability studies mentioned, the influence of an external vacuum was also investigated. Such an external vacuum constitutes a doubly connected domain of arbitrary shape for which the construction of a conformal mapping to an annular region greatly simplifies the stability analysis. This mapping problem was studied in the past as well in connection with the wing design of biplanes [13]. Here, the counterpart of Theodorsen's integral equation is Garrick's integral equation for which Henrici's method works as well. A double set of Fourier coefficients is now exploited, corresponding to the Laurent series expansion of analytic functions in an annulus. We will not discuss this method further since it has been extensively described in Ref. [4]. Again, it could profitably be exploited in vortex dynamics of incompressible flow in annular domains, as studied, e.g., in Ref. [14].

2.3. *Inner Products*

We will now fix a set of two-dimensional expansion functions

$$S_{mn}(s, \tau) \equiv R_{mn}(s)e^{im\tau}, \tag{25}$$

according to the conditions outlined in Section 2.1. This is mainly dictated by the choice of an inner product for these functions. However, we recall that the actual physics is determined by the velocity vector field $\mathbf{v}$. Since the accurate representation of the kinetic energy is of crucial importance, both in linear stability of tokamaks and in nonlinear vortex dynamics, the most relevant normalization of these variables is the following one:

$$K = \frac{1}{2}\int \rho|\mathbf{v}|^2\, dV = \|\mathbf{v}\|^2 = \langle \mathbf{v}, \mathbf{v}\rangle_{(2V)}. \tag{26}$$

Here, the index (2V) indicates that the inner product refers to 2D vectors. We will also introduce an inner product for 2D scalars, like the stream function $S(s, \tau)$, indicated by the index (2S), and an inner product for 1D functions, like the expansion functions $R_{mn}(s)$, indicated by the index (1). However, these additional definitions will be completely determined by the choice for the 2D vector inner product.

Let us exploit dimensionless variables by dividing out the total volume $V = \pi a^2 L$, where a measures the radial size of the domain and L the size in the ignorable direction, and the density ρ, which is assumed to be constant. The relevant inner product for 2D vectors may then be defined as

$$\langle \mathbf{v}_1, \mathbf{v}_2\rangle_{(2V)} \equiv \frac{1}{2\pi}\int_0^1 \int_0^{2\pi} \mathbf{v}_1^* \cdot \mathbf{v}_2 h^2 s\, ds\, d\tau. \tag{27}$$

The resulting definition for the inner product of 2D scalars reads

$$\langle S_1, S_2\rangle_{(2S)} \equiv \frac{1}{2\pi}\int_0^1\int_0^{2\pi}\left(\frac{1}{s^2}\frac{\partial S_1^*}{\partial\tau}\frac{\partial S_2}{\partial\tau}+\frac{\partial S_1^*}{\partial s}\frac{\partial S_2}{\partial s}\right)s\,ds\,d\tau, \tag{28}$$

and for 1D functions

$$\langle R_1, R_2\rangle_{(1)} \equiv \int_0^1\left[\frac{m^2}{s^2}R_1(s)R_2(s)+R_1'(s)R_2'(s)\right]s\,ds, \tag{29}$$

where the prime denotes differentiation with respect to s. Note how the latter two inner products have become independent of the scale factor of the conformal mapping. In the last definition, the appearance of the constant m betrays the two-dimensional origin of this inner product. Clearly, these 1D radial functions are always to be considered together with the angular factors $e^{im\tau}$.

We will now demand the 1D expansion functions $R_{mn}(s)$ to be orthonormal with respect to the inner product (29):

$$\langle R_{mn}, R_{m\nu}\rangle_{(1)} = \int_0^1\left[\frac{m^2}{s^2}R_{mn}(s)R_{m\nu}(s)+R_{mn}'(s)R_{m\nu}'(s)\right]s\,ds = \delta_{n\nu}. \tag{30}$$

This implies that the 2D expansion functions $S_{mn}(s,\tau)$, defined by Eq. (25), will be orthonormal with respect to the inner product (28):

$$\langle S_{mn}, S_{\mu\nu}\rangle_{(2S)} = \delta_{m\mu}\delta_{n\nu}. \tag{31}$$

Consequently, the inner product of two stream functions S_1 and S_2 expressed as in Eq. (11) will be given by the diagonal sum

$$\langle S_1, S_2\rangle_{(2S)} = \sum_{m=-\infty}^{\infty}\sum_{n=0}^{\infty}\sigma_{1,mn}^*\sigma_{2,mn}. \tag{32}$$

Similarly

$$K = \langle \mathbf{v}, \mathbf{v}\rangle_{(2V)} = \langle S, S\rangle_{(2S)} = \sum_{m=-\infty}^{\infty}\sum_{n=0}^{\infty}|\sigma_{mn}|^2. \tag{33}$$

In this manner, both the vector character of the flow and the stream function constraint (2) are fully exploited.

The 2D structure of the problem may be articulated some more by considering the expansion of the radial and angular components of the velocity in s,τ coordinates,

$$\begin{aligned} hv_s(s,\tau) &= \sum_{m=-\infty}^{\infty}\sum_{n=0}^{\infty}\sigma_{mn}X_{mn}(s)e^{im\tau},\\ hv_\tau(s,\tau) &= \sum_{m=-\infty}^{\infty}\sum_{n=0}^{\infty}\sigma_{mn}Y_{mn}(s)e^{im\tau}, \end{aligned} \tag{34}$$

where the functions

$$X_{mn}(s) \equiv (m/s)R_{mn}(s), \quad Y_{mn}(s) \equiv R'_{mn}(s) \tag{35}$$

would represent the radial and angular parts of expansion *vector* functions. Both contribute to the inner product of the 1D expansion functions, which may be written as

$$\langle R_{mn}, R_{m\nu}\rangle_{(1)} = \int_0^1 [X_{mn}(s)X_{m\nu}(s) + Y_{mn}(s)Y_{m\nu}(s)]s\, ds = \delta_{n\nu}. \tag{36}$$

Parenthetically, it should be noted that the expansion functions $R_{mn}(s)$, and their companions $X_{mn}(s)$ and $Y_{mn}(s)$, could also be exploited to represent compressible fluid flow. Two *different* sets of expansion coefficients, σ_{mn} and τ_{mn}, should then be used in Eq. (34) for the representation of v_s and v_τ.

In Section 3, we will construct the functions R_{mn} explicitly, based on the inner product (30).

3. ORTHOGONAL POLYNOMIALS

3.1. *Boundary Conditions and Reduction to Standard Form*

We wish to construct the polynomial representation of the 1D expansion functions $R_{mn}(s)$, based on the orthonormality condition (30) and satisfying simple boundary conditions at $s = 0$ and $s = 1$. Since the inner product definition (29) is not of a standard type, we need to perform some analysis to produce the explicit expressions and to obtain the relationships with standard (Jacobi) polynomials.

With respect to the boundary conditions, we impose the following constraints on the polynomials:

(1) Close to the origin $s = 0$, we demand radial behavior of $R_{mn}(s)$ consistent with the angular factors $e^{im\tau}$, i.e.,

$$R_{mn} \sim s^{|m|} \quad (s \ll 1); \tag{37}$$

(2) At the boundary $s = 1$, we permit two kinds of boundary conditions, corresponding to either fixed or free boundaries. For fixed boundary problems, we demand vanishing of the normal velocity component corresponding to each R_{mn} separately, i.e.,

$$\mathbf{n}\cdot\mathbf{v}|_{s=1} = v_s = -\frac{1}{hs}\frac{\partial S_{mn}}{\partial \tau}\bigg|_{s=1} = 0 \Rightarrow R_{mn}(1) = 0 \quad (n \geq 1). \tag{38}$$

Hence, to satisfy the fixed boundary condition, there is no need for superposition! For free boundary problems, the normal velocity component $\mathbf{n}\cdot\mathbf{v}$ should attain prescribed values $\neq 0$ at the boundary. This is affeced by extending the set $\{R_{mn}\}$ with one additional function R_{m0} for each value of m, such that

$$R_{m0}(1) \neq 0, \tag{39}$$

whereas the remaining R_{mn}'s should still satisfy Eq. (38). In this case, superposition of the R_{m0}'s is needed to produce the prescribed boundary values of $\mathbf{n}\cdot\mathbf{v}$.

Surprisingly, these restrictive conditions still admit two distinct classes of solutions, to be called orthogonal polynomials of the first and of the second class. We will discuss both of them.

We implement the condition (37) by writing

$$R_{mn}(s) \equiv s^{|m|} T_{mn}(s), \tag{40}$$

where the T_{mn}'s are auxiliary polynomials that facilitate the reduction of the inner product (30) to a standard expression after integration by parts:

$$\langle R_{mn}, R_{m\nu}\rangle_{(1)} = \int_0^1 s^{2|m|+1} T'_{mn}(s) T'_{m\nu}(s)\, ds + |m| T_{mn}(1) T_{m\nu}(1) = \delta_{n\nu}. \tag{41}$$

Hence, the condition (39) for the free-boundary components may be satisfied by the choice

$$T_{m0}(s) = \text{const} = |m|^{-1/2}, \tag{42}$$

whereas the condition (38) for the fixed-boundary components is then satisfied by imposing $T_{mn}(1) = 0$ so that the inner product reduces to

$$\int_0^1 s^{2|m|+1} T'_{mn}(s) T'_{m\nu}(s)\, ds = \delta_{n\nu} \quad (n, \nu \neq 0). \tag{43}$$

The latter expression is now of a standard type so that the T'_{mn}'s may be written as Jacobi polynomials [15]:

$$\begin{aligned} T'_{mn}(s) &= \frac{(2|m|+2n-1)!\sqrt{2(|m|+n)}}{(n-1)!(2|m|+n)!} G_{n-1}(2|m|+2, 2|m|+2, s) \\ &= \sqrt{2(|m|+n)} \sum_{\lambda=1}^{n} \frac{(-1)^{\lambda-1}(2|m|+2n-\lambda)!}{(\lambda-1)!(n-\lambda)!(2|m|+n-\lambda+1)!} s^{n-\lambda} \quad (n \neq 0). \end{aligned} \tag{44}$$

Integration produces the explicit expressions for the polynomials $T_{mn}(s)$ themselves so that the polynomials $R_{mn}(s)$ are determined as well.

The auxiliary polynomials $T_{mn}(s)$ just produced consist of even and odd powers of s. The associated orthogonal polynomials $R_{mn}(s)$ will be called polynomials of the first class. As mentioned above, another set can be derived that also satisfies all of the formulated conditions. They will be called orthogonal polynomials of the second class and designated with a tilde. Their existence is evident from the expression (43) which may be transformed to even powers of s by introducing the variable $\xi = s^2$ so that the orthonormality condition becomes

$$2 \int_0^1 \xi^{|m|+1} \frac{d\tilde{T}_{mn}}{d\xi} \frac{d\tilde{T}_{m\nu}}{d\xi}\, d\xi = \delta_{n\nu}. \tag{45}$$

Hence, the expression for $d\tilde{T}_{m\nu}/d\xi$ may be obtained from Eq. (44) by applying the transformations

$$T'_{mn} \to \sqrt{2}\, d\tilde{T}_{mn}/d\xi, \quad s \to \xi, \quad 2|m| \to |m|. \tag{46}$$

Integration provides $\tilde{T}_{mn}$ and, returning to the variable s again, the explicit expressions for the polynomials $\tilde{R}_{mn}(s)$ of the second class. The transformation (46) implies the following relationship between the two sets of polynomials,

$$\tilde{R}_{2m,n}(s) = \frac{1}{\sqrt{2}} R_{mn}(s^2), \tag{47}$$

i.e., the m-polynomials of the first class relate to the $2m$-polynomials of the second class. Since the polynomials always have to be considered together with their angular factors, this shows that the associated 2D expansion functions $S_{mn}(s,\tau)$ and $\tilde{S}_{mn}(s,\tau)$ are really two different sets.

Maybe not too surprising, properly scaled Bessel functions also satisfy the orthonormality condition (30) and the boundary conditions (37) and (38). Moreover, they can be extended with the same free-boundary functions as the polynomials R_{mn} and $\tilde{R}_{mn}$. Distinguishing them with a circumflex, they read

$$\begin{aligned} \hat{R}_{m0}(s) &= |m|^{-1/2} s^{|m|} \quad (\equiv R_{m0}(s) \equiv \tilde{R}_{m0}(s)), \\ \hat{R}_{mn}(s) &= \frac{\sqrt{2}}{j_{mn} J_{m-1}(j_{mn})} J_m(j_{mn} s) \quad (n \geq 1), \end{aligned} \tag{48}$$

where j_{mn} indicates the successive zeros of J_m. The reason to prefer the polynomials $R_{mn}(s)$ and $\tilde{R}_{mn}(s)$ in the numerics is that they are much easier to manipulate and that they obviate the task of having to compute all those zeros.

In order to exploit the polynomials $R_{m\nu}$ and $\tilde{R}_{m\nu}$, all their properties should be derived. This involves considerable and, as noted by one author [16], rather addictive algebra that will not be presented here. The results are just stated in Sections 3.2 and 3.3.

3.2. *Polynomials of the First Class*

The explicit expressions for the polynomials of the first class read, for $n = 0$,

$$R_{m0}(s) = |m|^{-1/2} s^{|m|}, \tag{49}$$

and for $n \geq 1$,

$$R_{mn}(s) = \sqrt{2(|m|+n)}\, s^{|m|} \sum_{\lambda=1}^{n} \frac{(-1)^\lambda (2|m|+2n-\lambda)!}{(\lambda-1)!(n-\lambda+1)!(2|m|+n-\lambda+1)!} (1 - s^{n-\lambda+1}). \tag{50}$$

They satisfy the recursion relation

$$\begin{aligned} R_{mn} = -\frac{2|m|+2n-1}{n(2|m|+n)} \Bigg[\left\{ \frac{(2|m|+n-1)^2 + n(n-2)}{(2|m|+2n-1)(2|m|+2n-3)} - s \right\} (2|m|+2n-2) \\ \times \sqrt{\frac{|m|+n}{|m|+n-1}} R_{mn-1} + \frac{(n-2)(2|m|+n-2)}{2|m|+2n-3} \sqrt{\frac{|m|+n}{|m|+n-2}} R_{mn-2} \Bigg], \end{aligned} \tag{51}$$

the differential relation

$$R'_{mn} = \frac{1}{s(1-s)}\left[\left\{\frac{|m|(2|m|+2n-1)+n(n-1)}{(|m|+n)(2|m|+2n-1)} - s\right\}(|m|+n)R_{mn} + \frac{(n-1)(2|m|+n-1)}{2|m|+2n-1}\sqrt{\frac{|m|+n}{|m|+n-1}}R_{mn-1}\right], \tag{52}$$

and the differential equation

$$R''_{mn} + \frac{1}{s}R'_{mn} - \left[\frac{m^2}{s^2} - \frac{n(2|m|+n)}{s(1-s)}\right]R_{mn} = 0. \tag{53}$$

Their computation is extremely fast and accurate: The first two polynomials R_{m1} and R_{m2} are computed from the explicit expression (50) and all the higher order polynomials $R_{mn}(n \geq 3)$ from the recursion relation (51), the derivatives R'_{mn} from the differential relation (52), and, if they are needed, the second order derivatives from the differential equation (53).

The lowest polynomials of the first class are plotted in Fig. 2. As compared to the Bessel functions (48), their zeros are located somewhat more to the right. Another difference occurs for the $m = 0$ polynomials, which do not have a vanishing derivative at $s = 0$: $R'_{0n}(0) \neq 0$, whereas $\hat{R}'_{0n}(0) = 0$. Clearly, if this property is essential for the proper representation of variables it will be produced automatically in the numerics by sums of pairs of R_{0n}'s.

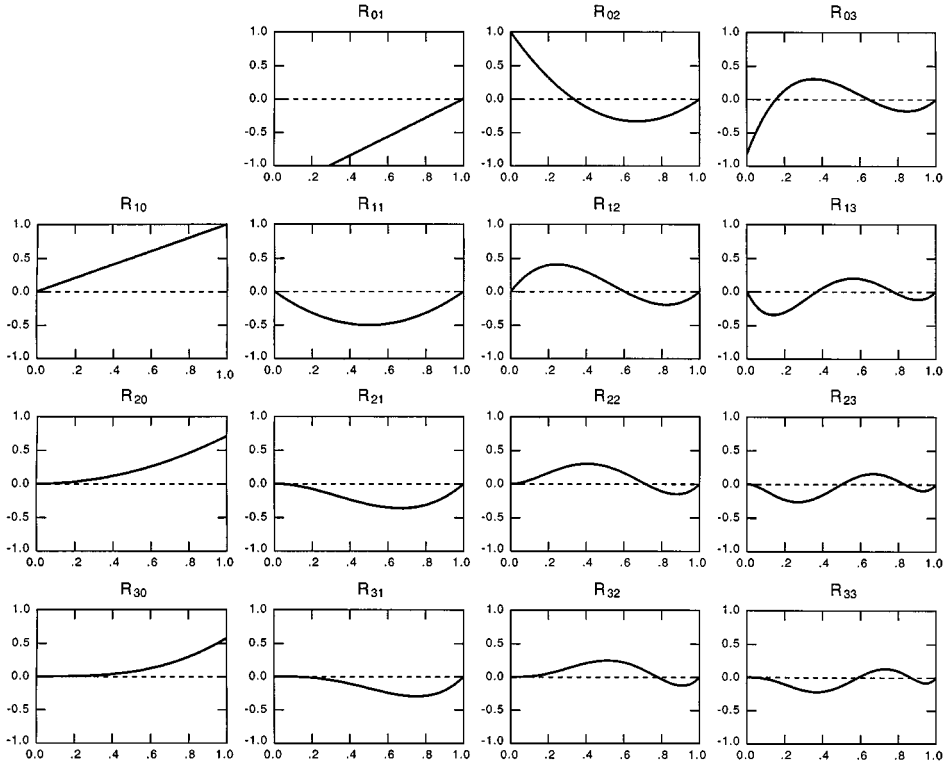

FIG. 2. Orthogonal polynomials of the first class.

3.3. *Polynomials of the Second Class*

The explicit expressions for the polynomials of the second class read, for $n=0$,

$$\tilde{R}_{m0}(s) = |m|^{-1/2} s^{|m|}, \tag{54}$$

and for $n \geq 1$,

$$\tilde{R}_{mn}(s) = \sqrt{\frac{|m|+2n}{2}}\, s^{|m|} \sum_{\lambda=1}^{n} \frac{(-1)^{\lambda}(|m|+2n-\lambda)!}{(\lambda-1)!(n-\lambda+1)!(|m|+n-\lambda+1)!}\left(1-s^{2(n-\lambda+1)}\right). \tag{55}$$

They satisfy the recursion relation

$$\tilde{R}_{mn} = -\frac{|m|+2n-1}{n(|m|+n)}\left[\left\{\frac{(|m|+n-1)^2+n(n-2)}{(|m|+2n-1)(|m|+2n-3)} - s^2\right\}(|m|+2n-2) \times \sqrt{\frac{|m|+2n}{|m|+2n-2}}\,\tilde{R}_{mn-1} + \frac{(n-2)(|m|+n-2)}{|m|+2n-3}\sqrt{\frac{|m|+2n}{|m|+2n-4}}\,\tilde{R}_{mn-2}\right], \tag{56}$$

the differential relation

$$\tilde{R}'_{mn} = \frac{1}{s(1-s^2)}\left[\left\{\frac{|m|(|m|+2n-1)+2n(n-1)}{(|m|+2n)(|m|+2n-1)} - s^2\right\}(|m|+2n)\,\tilde{R}_{mn} + \frac{2(n-1)(|m|+n-1)}{|m|+2n-1}\sqrt{\frac{|m|+2n}{|m|+2n-2}}\,\tilde{R}_{mn-1}\right], \tag{57}$$

and the differential equation

$$\tilde{R}''_{mn} + \frac{1}{s}\tilde{R}'_{mn} - \left[\frac{m^2}{s^2} - \frac{4n(|m|+n)}{1-s^2}\right]\tilde{R}_{mn} = 0. \tag{58}$$

They are computed in the same manner as the polynomials of the first class.

The lowest polynomials of the second class are plotted in Fig. 3. As compared to the polynomials of the first class, their zeros are moved even further to the right so that they are further away from the Bessel functions (48) in that respect. On the other hand, the $m=0$ polynomials of the second class do have a vanishing derivative at the origin: $\tilde{R}'_{0n}=0$.

Finally, the unavoidable question on which of the two kinds of polynomials is to be preferred in the numerics cannot be answered in general terms. The answer to this question appears to depend on where the physical phenomena tend to be localized and on what integration scheme is exploited. Our experience with stability codes indicates that the two sets are equally good for that purpose.

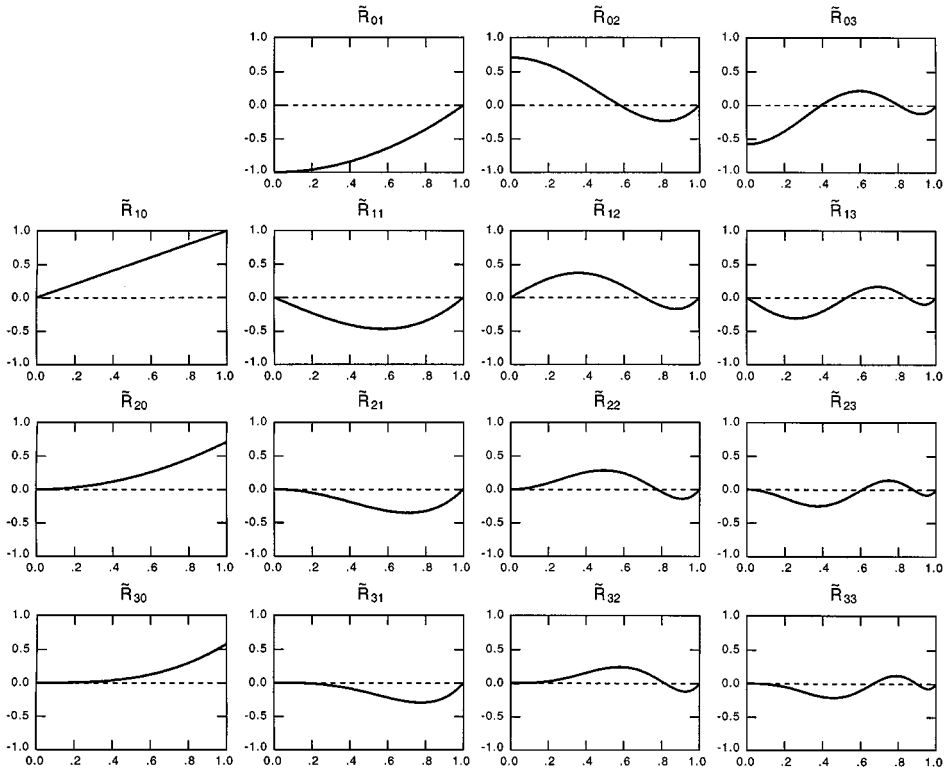

FIG. 3. Orthogonal polynomials of the second class.

4. CONCLUSIONS

We have constructed two sets of two-dimensional expansion functions $S_{mn}(s,\tau) \equiv R_{mn}(s)e^{im\tau}$ and $\tilde{S}_{mn}(s,\tau) \equiv \tilde{R}_{mn}(s)e^{im\tau}$ for the representation of the stream function of incompressible 2D flow on an arbitrary domain, exploiting an inner product that is based on the kinetic energy of the velocity field of the flow. The coordinates s and τ refer to a computational w-plane obtained from the physical z-plane by conformal mapping, where the physical boundary is mapped onto a circle in the w-plane. Since such a mapping needs to be constructed only once during the computation and since it can be obtained with one-dimensional accuracy (basically, it is just a way of computing a Cauchy integral along the boundary curve), this transformation represents negligible overhead in the numerical calculations. The one-dimensional expansion functions $R_{mn}(s)$ and $\tilde{R}_{mn}(s)$ are orthogonal polynomials with respect to a nonstandard inner product that derives directly from the kinetic energy of the associated 2D velocity components. Moreover, the velocity components associated with a single polynomial satisfy regularity conditions at the origin ($s=0$) and either fixed boundary conditions at the boundary ($s=1$), for the $n \neq 0$ components, or free-boundary conditions, for the $n=0$ components. In this manner, the physical structure of vortex dynamics in two dimensions is optimally expressed in the separate expansion functions: For the fixed boundary case, coupling will only occur through inhomogeneities and nonlinearities, not through the boundary conditions!

The expansion functions exploited by Verkley [1] do not have these properties since they are based on a standard inner product for the 1D functions, so that the associated

normalization of the velocities will not correspond to the kinetic energy. They also do not satisfy the boundary conditions separately, but require superposition. These features might enhance the reported problem of nonconservation of energy for the truncated polynomial representation which comes about from the nonlinear advection term $\{S, \nabla^2 S\}$ of Eq. (4). This term vanishes for Besselfunction representations $\hat{S}_{mn} \equiv \hat{R}_{mn} e^{im\tau}$, with $\hat{R}_{mn}$ given by Eq. (48):

$$\{\hat{S}_{mn}, \nabla^2 \hat{S}_{mn}\} = j_{mn}^2 \{\hat{S}_{mn}, \hat{S}_{mn}\} = 0. \tag{59}$$

It does not vanish for the polynomial representation used in [1]. Our expansion functions S_{mn} and $\tilde{S}_{mn}$ do not eliminate this term either since they are not eigenfunctions of the Laplacian, as follows from the differential equations (53) and (58) for R_{mn} and $\tilde{R}_{mn}$. However, they do not produce additional higher order terms through the boundary conditions.

In the tokamak stability calculations [2–8], the expansion functions S_{mn} and $\tilde{S}_{mn}$ automatically avoid the problem of spectral pollution [17] because of the built-in balance of the representation of the normal and tangential velocity components. Moreover, conformal mapping can be replaced by other kinds of mappings that may be more relevant for the physics of the problem, like the much exploited system of nonorthogonal flux coordinates with a straight field line representation. Here, s and τ are replaced by $\sqrt{\psi}$ and ϑ, where ψ is the poloidal magnetic flux and ϑ is a poloidal angle constructed such that the magnetic field lines become straight in the $\psi - \vartheta$ plane. Expansion functions $S_{mn}(\sqrt{\psi}, \vartheta)$ and $\tilde{S}_{mn}(\sqrt{\psi}, \vartheta)$, with the same orthogonal polynomials of the first and second class, have been successfully exploited [6, 7], even though the kinetic energy is necessarily nondiagonal in that case.

We conclude that the constructed polynomials are perfectly suited for numerical calculations and computer algebra of vortex dynamics.

ACKNOWLEDGMENTS

This work was performed as part of the research program of the association agreement of Euratom and the "Stichting voor Fundamenteel Onderzoek der Materie" (FOM) with financial support from the "Nederlandse Organisatie voor Wetenschappelijk Onderzoek" (NWO) and Euratom.

REFERENCES

1. W. T. M. Verkley, A Spectral model for two-dimensional incompressible fluid flow in a circular basin. I, II, *J. Comput. Phys.* **136**, 100 (1997); **136**, 115 (1997).
2. J. P. Freidberg and J. P. Goedbloed, Equilibrium and stability of a diffuse high-beta tokamak, in *Pulsed High Beta Plasmas*, edited by Evans (Pergamon Press, Oxford, 1976), p. 117.
3. J. P. Goedbloed, Conformal mapping methods in two-dimensional magnetohydrodynamics, *Comp. Phys. Comm.* **24**, 311 (1981).
4. J. P. Goedbloed, Free-boundary high-beta tokamaks. I, II, III, *Phys. Fluids* **25**, 852 (1982); **25**, 2062 (1982); **25**, 2073 (1982).
5. J. P. Goedbloed, G. M. D. Hogewey, R. Kleibergen, J. Rem, R. M. O. Galvão, and P. H. Sakanaka, Investigation of high-beta tokamak stability with the program HBT, in *Proc. Tenth International IAEA Conference on Plasma Physics and Controlled Fusion Research, London, 12–19 September 1984* (IAEA, Vienna, 1985), Vol. 2, p. 165.

6. J. P. Goedbloed, R. Kleibergen, and J. Rem, Flux coordinate studies of elongated plasmas at high beta, in *Proc. 14th European Conference on Controlled Fusion and Plasma Physics, Madrid, June 22–26, 1987* (EPS, 1987), Vol. III, p. 1095.
7. R. Kleibergen and J. P. Goedbloed, Alfvén wave spectrum of an analytic high-beta tokamak equilibrium, *Plasma Phys. Contr. Fusion* **30**, 1961 (1988).
8. G. T. A. Huysmans, T. C. Hender, O. J. Kwon, J. P. Goedbloed, E. Lazzaro, and P. Smeulders, MHD stability analysis of high-β JET discharges, *Plasma Phys. Contr. Fusion* **34**, 487 (1992).
9. T. Theodorsen, NACA Report 411 (1931).
10. M. H. Gutknecht, Existence of a solution of the discrete Theodorsen equation for conformal mappings, *Math. Comput.* **31**, 478 (1977).
11. P. Henrici, Fast Fourier methods in computational complex analysis, *SIAM Rev.* **21**, 481 (1979).
12. P. Henrici, *Applied and Computational Complex Analysis. Vol. 3 Discrete Fourier Analysis-Cauchy Integrals-Construction of Conformal Maps-Univalent Functions* (Wiley, New York, 1986).
13. T. Garrick, *Potential Flow about Arbitrary Biplane Wing Sections*, NACA Report 542 (1936).
14. M. Elghaoui and R. Pasquetti, Mixed spectral-boundary element embedding algorithms for the Navier–Stokes equations in the vorticity-stream function formulation, *Comput. Phys.* **153**, 82 (1999).
15. M. Abramowitz and I. A. Segun, *Handbook of Mathematical Functions* (Dover, New York, 1968).
16. J. Riordan, *Combinatorial Identities* (Wiley, New York, 1968).
17. R. Gruber and J. Rappaz, *Finite Element Methods in Linear Ideal Magnetohydrodynamics* (Springer-Verlag, Berlin, 1985).